Accounts

Structure Analysis of Reaction Intermediates in Metal Substitution Reactions in Solution by the Stopped-Flow EXAFS Method

Kazuhiko Ozutsumi and Hitoshi Ohtaki*

Department of Chemistry, Faculty of Science and Engineering, Ritsumeikan University, 1-1-1 Noji-Higashi, Kusatsu 525-8577

(Received March 23, 1999)

Improvements of XAFS (X-Ray Absorption Fine Structure) measurements in the time domain are summarized and several examples of structure determination of reaction intermediates by the EXAFS (Extended X-Ray Absorption Fine Structure) method are given. The local structure around the copper(II) or cobalt(II) ion is described in the reaction intermediate in the metal substitution reaction of the homodinuclear mercury(II) porphyrinato (5,10,15,20-tetrakis(4-sulfonatophenyl)porphyrin; H_6tpps) complex in an acetate buffer determined by the stopped-flow EXAFS (SF-EXAFS) method, which was developed by us. Comparison of the bond lengths in the intermediates with those in the reactants and the products of the metal substitution reaction, the structure of which has been determined by the same method, revealed the cause of the instability of the reaction intermediates.

Structures of stable species in solution are now routinely analyzed by the solution X-ray diffraction and/or EXAFS (Extended X-Ray Absorption Fine Structure) methods. Such structural information is essential to elucidate the static behavior of chemical reactions in solution, i.e., thermodynamic properties are reasonably explained based on the microscopic structure of solutions. However, reaction processes have usually been studied kinetically and dynamically. Studies of reaction mechanisms often suggested the formation of short-lived reaction intermediates with elongated bonds at the reaction site and the structure of the intermediates was usually estimated from spectrophotometric data. Knowledge about the structure of reaction intermediates, such as bond lengths and the coordination number, is very important to elucidate reaction mechanisms. Therefore, direct structure analysis of reaction intermediates is necessary. To determine such structure parameters, solution X-ray diffraction and EXAFS measurements should be carried out within a certain time domain. Many people have attempted to study time-resolved structural analysis of reaction intermediates. However, structural information of reaction intermediates in the literature is very limited.

If one can select a suitable reaction system and apply an appropriate method in a given time domain to determine the structure of a reaction intermediate, variation of bond lengths between a reaction center and an entering or leaving atom and the coordination number of a short-lived reaction intermediate formed in the course of the chemical reaction can be obtained. Such structural information is invaluable to understand the reactivity of reaction intermediates and will allow us to develop novel chemical reactions by controlling well-designed reaction intermediates. Time-resolved structural determination should be more and more important in studies of reaction mechanisms and the structural analysis of reaction intermediates will be a very important subject in chemistry.

In this report we deal with the structure analysis of reaction intermediates by the XAFS (X-Ray Absorption Fine Structure) method. The solution X-ray diffraction method is not suitable for fast reactions at the present stage. A book about X-ray crystallographic measurements in the time domain[1] and the current topics and perspective[2] for time-resolved X-ray crystallography are good references for studies on reaction intermediates in a crystalline state. However, such references include no information about reaction intermediates in solution. In the present report we first describe briefly the background for the time-resolved structural analysis; then, some examples of the structural determination of reaction intermediates by the EXAFS method so far reported are reviewed. Finally, our results obtained by combining the EXAFS method with a stopped-flow technique, which has been developed by us, are presented.[3—6] The stopped-flow EXAFS (SF-EXAFS) method has been successfully applied to the determination of the local structure around the copper(II) or cobalt(II) ion in the short-lived reaction intermediate formed during the metal substitution reaction

of the homodinuclear mercury(II) porphyrinato (5,10,15, 20-tetrakis(4-sulfonatophenyl)porphyrin : H_6tpps) complex with copper(II) or cobalt(II) ion in an acetate buffer. We compare the bond lengths in the intermediates with those in the reactants and the products of the metal substitution reaction and discuss the instability of the reaction intermediates.

1. XAFS Measurements in the Time Domain

In an early stage of the development of measurements of XAFS spectra in the time domain, the energy-dispersive method was examined.[7—10] Use of an X-ray dispersive geometry and a position-sensitive detector makes simultaneous measurement at many data points possible and one could easily expect that the energy-dispersive mode is suitable for fast measurement of XAFS spectra. By combining an energy-dispersive type XAFS spectrometer with an X-ray film and then with an electronic linear photodiode array detector, one can obatin an EXAFS spectrum with the measurement time less than 1 s. From a practical point of view, a time scale of ca. 100 ms can be used.

Energy-dispersive XAFS experiments had been examined by combining a stopped-flow technique in 1986.[11] XANES (X-Ray Absorption Near Edge Structure) spectra for the reduction process of Fe(III) by hydroquinone were recorded with a time resolution of 25 ms. Later, the time resolution was improved to 5 ms and this method was employed to study the fast reactions of Fe(III) with catechol or thiosulfate as well as with hydroquinone.[12,13] The time-resolved EXAFS measurement was demonstrated for the Fe(III)-thiosulfate system.[12] However, although all of the experiments could follow changes of XANES and EXAFS spectra with time, the works were unsuccessful in obtaining the relevant spectra of reaction intermediates.

The energy-dispersive method is essentially applicable to transmission experiments. Dilute samples such as many protein solutions must be measured by the fluorescent detection in combination with an angular-dispersive XAFS spectrometer, despite a disadvantage originating from an angle scan of the monochromator crystal. A new concept for time-resolved measurement was presented using the angular-dispersive method, i.e., by synchronizing a pulsed laser with an SR (synchrotron radiation) pulse in the single bunch mode, time resolution variable from nanoseconds to 1000 μs was achieved.[14] Then, 100 μs resolved XANES spectra of photolyzed carboxymyoglobin were measured for the first time.[15,16]

All attempts described above were made at SR facilities. This is because SR can supply a structureless X-ray spectrum with intense flux, small beam divergence and polarization. However, the use of SR facilities imposes some restrictions on users. Therefore, a laboratory-scale XAFS spectrometer is needed for daily research. The first in-laboratory XAFS spectrometer for measurement in the time domain was an energy-dispersive type using a self-scanning photodiode array.[3,4] Later, an angular-dispersive spectrometer with a solid-state detector was developed.[17] These spectrometers were combined with a stopped-flow unit and were successfully adopted to the structural determination of the reaction intermediates having a lifetime of a few seconds, which was limited by the low photon flux emitted from a rotating anode X-ray generator. It should be noted that the structural determination of reaction intermediates was successfully carried out not in the SR facility but in our laboratory.

Recently, SR was again employed as an X-ray source and the angular-dispersive method in transmission mode combined with a stopped-flow device was applied to the fast redox reaction of $[Fe(CN)_6]^{3-}$ with L-ascorbic acid in an acidic aqueous solution to check the time-resolution ability.[18] The shortest sampling time of the technique was found to be on the order of 1 ms; the rate constants derived from the time-resolved XANES spectra agreed well with those determined by UV-vis spectroscopy.[19] However, no structural data have been obtained for any species having such a lifetime.

2. Structure Analysis of Reaction Intermediates

To determine the structure of reaction intermediates, it is not always necessary to perform measurements in the time domain. A good example was shown by the structural determination of the photoexcited species of carboxymyoglobin (MbCO) at 4.2 K.[20,21] Steady irradiation increased the amount of the photoexcited species MbCO* up to 70% and EXAFS spectra were measured by a usual method. The Fe–N and Fe–C bond lengths in MbCO* are slightly longer by 3—5 pm than those in MbCO, showing the small displacement of the CO molecule on photolysis. Similarly, XAFS spectra of (η-cyclopentadienyl)nitrosylnickel(I), $[Ni(C_5H_5)(NO)]$, in 3-methylpentane solution were measured at 20 K.[22] The Ni–N and Ni–C distances in the ground state $[Ni(C_5H_5)(NO)]$ are 165 and 215 pm, respectively. By irradiating with 365 nm light, the photoexcited state $[Ni(C_5H_5)(NO)]^*$ was converted into the charge-transfer state $[Ni(C_5H_5)(NO)]^{CT}$. The analysis of the XAFS spectra revealed the conversion extent to the charge-transfer state $[Ni(C_5H_5)(NO)]^{CT}$ to be 43% and the Ni–N and Ni–C bond lengths to be 177 and 215 pm, respectively. The elongation of the Ni–N distance in $[Ni(C_5H_5)(NO)]^{CT}$ is reasonably explained by the decreased Ni–N bond order resulting from electron transfer from Ni to NO. Also, the linear Ni–N–O geometry in the ground state changes upon photoexcitation to become the bent configuration (Ni–N–O bond angle was estimated to be 142—152°).

In 1993, for the first time, two papers were published about the structure of reaction intermediates in a solution phase.[3,23] In both cases the XAFS measurements were performed in the time domain. One report concerns the structure of a short-lived excited species in solution.[23] By combining the fluorescent EXAFS method with the rapid-flow laser spectroscopy, the structure of the triplet excited species of $[Pt_2(P_2H_2O_5)_4]^{4-}$ with a lifetime of about 4 μs was determined at 16 °C. The 4.7 pm contraction in the Pt–P bond length in the excited species was found relative to that in the ground state structure. A drastic change occurred in the Pt···Pt distances. In the excited state, the Pt···Pt distance is much shorter, by 52 pm, than that in the ground

state. However, such analytical results should involve very large uncertainties because the amount of the photoexcited species formed does not exceed 18%, which is almost a limit or out of limit of concentration suitable for structural determination. The other report[3] presented the structure of the heterodinuclear reaction intermediate, $[Hg(tpps)Cu]^{2-}$, details of which will be described in the following section. The intermediate is formed during the metal substitution reaction of the homodinuclear mercury(II) porphyrinato complex with copper(II) ion.

$$[Hg_2(tpps)]^{2-} + Cu^{2+} \longrightarrow [Hg(tpps)Cu]^{2-} + Hg^{2+} \longrightarrow [Cu(tpps)]^{4-} + 2Hg^{2+} \quad (1)$$

In Eq. 1 the formation of the intermediate reached almost 100% under a suitable condition and the EXAFS spectra were measured by an in-laboratory energy-dispersive spectrometer combined with a stopped-flow apparatus. This may be the first successful determination of the structure of a reaction intermediate with reasonable accuracy.

Much effort has been devoted to develop instruments, but only a limited number of successful structure determinations of reaction intermediates have been reported. Success in measuring time-resolved EXAFS spectra of good quality does not always mean successful structural determination of reaction intermediates. The amount of intermediate formed is essentially important, regardless of the lifetime of intermediates. Thus, sufficient knowledge of both reaction kinetics and XAFS measurements is necessary. The selection of suitable systems to determine the structure of intermediates must be done on the basis of sound knowledge of solution chemistry.

A further example is the structural determination of the peroxochromium(VI) intermediate which appears during the reduction process of Cr(VI) by hydrogen peroxide.[24]

$$HCrO_4^- + 2H_2O_2 + H^+ \rightleftarrows CrO(O_2)_2 + 3H_2O \quad (2)$$

$$2CrO(O_2)_2 + 6H^+ \rightleftarrows 2Cr^{3+} + 3O_2 + H_2O_2 + 2H_2O \quad (3)$$

The structure of the reaction intermediate, $[CrO(O_2)_2]$, was determined by using an angular-dispersive spectrometer combined with a stopped-flow unit. The Cr(IV) center in the intermediate is coordinated with one oxo group, two peroxo groups, and one water molecule. The six-coordinate pentagonal pyramidal structure of the intermediate was proposed.

3. Structure of the Reaction Intermediates Formed in the Metal Substitution Reaction of the Mercury(II) Porphyrinato Complex

3. 1. Formation of Reaction Intermediates. The rates of formation of metalloporphyrins are usually very slow. However, the addition of large metal ions such as mercury(II), cadmium(II), and lead(II) accelerates the metallation of medium-sized metal(II) ions.[24] We used 5,10,15,20-tetrakis(4-sulfonatophenyl)porphyrin : H_6tpps because of its high solubility in water. The following reaction mechanism has been proposed for the catalytic action of mercury(II):[25,26]

$$[Hg_2(tpps)]^{2-} \underset{k_{-1}}{\overset{k_1}{\rightleftarrows}} [Hg(tpps)]^{4-} + Hg^{2+} \quad (4)$$

$$[Hg(tpps)]^{4-} + M^{2+} \xrightarrow{k_2} [Hg(tpps)M^{II}]^{2-} \xrightarrow{k_3} [M^{II}(tpps)]^{4-} + Hg^{2+} \quad \text{(Final product)} \quad (5)$$

The large mercury(II) ion cannot accommodate in the porphyrin ring and sits above and below the porphyrin ring to form the homodinuclear mercury(II) complex. The dinuclear complex partially dissociates to the mononuclear complex and the hydrated mercury(II) ion. Then the mononuclear complex reacts with metal(II) ion to form the heterodinuclear intermediate, which decomposes to the metal(II) porphyrinato complex and the hydrated mercury(II) ion. The rate constants at 25 °C are practically independent of the nature of the incoming metal ions:[25,26] e.g., $k_1 = 1.95\times10^8$ mol^{-1} dm^3 s^{-1}, $k_2/k_{-1} = 7.14$ and $k_3 = 1.00\times10^{-2}$ s^{-1} for copper(II) and $k_1 = 1.02\times10^8$ mol^{-1} dm^3 s^{-1}, $k_2/k_{-1} = 0.14$ and $k_3 = 1.09\times10^{-2}$ s^{-1} for zinc(II).

For the copper(II) system, in the absence of any catalysts the metallation is very slow.

$$Cu^{2+} + H_2tpps^{4-} \xrightarrow{\text{very slow}} [Cu(tpps)]^{4-} + 2H^+ \quad (6)$$

In the presence of mercury(II), the copper(II) ion rapidly forms the $[Cu(tpps)]^{4-}$ complex through the formation of the heterodinuclear $[Hg(tpps)Cu]^{2-}$ reaction intermediate.

$$[Hg(tpps)]^{4-} + Cu^{2+} \xrightarrow{k_2} [Hg(tpps)Cu]^{2-} \xrightarrow{k_3} [Cu(tpps)]^{4-} + Hg^{2+} \quad (7)$$

It is reasonable to assume from the kinetic data that the short-lived heterodinuclear intermediate $[Hg(tpps)Cu]^{2-}$ formed on mixing a solution containing the mercury(II) porphyrinato complex with an aqueous solution of copper(II). The amount of the intermediate increases up to 100% in a time range which is suitable for our measurements by the SF-EXAFS apparatus. Thus, the structure determination of the reaction intermediate was examined by the SF-EXAFS method. The structure of the reactant (Cu^{2+} in an acetate buffer) and the product ($[Cu(tpps)]^{4-}$) was determined by the same method as employed for the intermediate in order to compare the structures of these complexes.

With cobalt(II), the $[Co^{II}(tpps)]^{4-}$ complex is formed as the product, but the complex is further oxidized by dissolved oxygen to $[Co^{III}(tpps)]^{3-}$.

$$Co^{2+} + H_2tpps^{4-} \xrightarrow{\text{very slow}} [Co^{II}(tpps)]^{4-} + 2H^+ \xrightarrow{O_2,\ \text{slow}} [Co^{III}(tpps)]^{3-} \quad (8)$$

The rate of the metallation is much slower than that of the oxidation, and hence, the determination of structural parameters of the $[Co^{II}(tpps)]^{4-}$ complex is impossible by the usual EXAFS method owing to the slow rate of the reaction and

the small amount of formation of the complex. Since the presence of a small amount of mercury(II) as catalyst enhances the formation rate of the $[Co^{II}(tpps)]^{4-}$ complex, we can employ the laboratory-scale SF-EXAFS method in the determination of the structure of not only the reaction intermediate, $[Hg(tpps)Co^{II}]^{2-}$, but also $[Co^{II}(tpps)]^{4-}$

$$[Hg(tpps)]^{4-} + Co^{2+} \xrightarrow{k_2} [Hg(tpps)Co^{II}]^{2-} \xrightarrow{k_3} [Co^{II}(tpps)]^{4-} + Hg^{2+} \xrightarrow{O_2,\ slow} [Co^{III}(tpps)]^{3-} \quad \text{(Final product)} \quad (9)$$

The structure of the $[Hg(tpps)Co^{II}]^{2-}$ intermediate is determinable by a similar procedure to that employed for the copper(II) system, because the formation process of the intermediate is not influenced by the kind of metal(II) ions. The oxidation process was checked by a preliminary experiment. We found that, in the presence of a small amount of mercury(II), the formation of the $[Co^{II}(tpps)]^{4-}$ complex reaches 100% within 300 s, and in the absence of an oxidant the cobalt(II) complex is preserved for at least 1500 s. However, the lifetime of the complex in air is too short to determine the structure of the complex by the usual procedure. The SF-EXAFS method is a useful tool for a structural determination of such an unstable species. The structure of the finally oxidized product, stable $[Co^{III}(tpps)]^{3-}$, was determined by using the same method.

3. 2. Sample Solutions. All chemicals of reagent grade were used without further purification. For the structure determination of the reaction intermediates, sample solutions listed in Table 1 were prepared.

An aqueous solution of copper(II) porphyrinate was prepared by mixing copper(II) acetate and H_6tpps which had been neutralized with a stoichiometric amount of NaOH in water, and then by heating the resultant solution on a water bath for several hours to complete the metallation reaction (solution CU-B). A cobalt(III) porphyrinate solution was prepared by a similar method by using cobalt(II) acetate and on the heating process cobalt(II) was oxidized to cobalt(III) by dissolved oxygen. The concentrations of the copper(II) and cobalt(III) ions in the solutions were 0.1 mol dm^{-3}.

Aqueous solutions of copper(II) sulfate, cobalt(II) perchlorate and hexaamminecobalt(III) chloride were prepared as structure standards for the EXAFS analysis. The concentrations of the metal ions were 0.2 mol dm^{-3} for copper(II) and 0.1 mol dm^{-3} for cobalt(II) and cobalt(III).

3. 3. SF-EXAFS Measurements. EXAFS spectra were measured around the copper or cobalt *K* edge on a laboratory EXAFS spectrometer of the energy dispersive type combined with a stopped-flow apparatus.[3,4] Molybdenum was used as the target of the X-ray source and a rotating anode X-ray generator (RU-300, Rigaku) was operated at the voltage of 12 kV and the current of 160 mA. A stopped-flow cell was located near the X-ray generator. Two windows, each having a thickness of 150 μm, of the stopped-flow cell were made of pyrolytically prepared boron nitride. A white X-ray beam was first passed through the stopped-flow cell and then reflected by a flat LiF(200) crystal. The resulting polychromatic X-rays were detected by a position-sensitive self-scanning photodiode array (S3904-1024Q, Hamamatsu Photonics).

X-Ray intensities I_0 and I transmitted through the stopped-flow cell filled with water and a sample solution, respectively, were measured for a given time of opening of the shutter (gate time). Before measuring transmitted intensities, the dark current of the photodiode array was measured for the same gate time and this value was subtracted from the transmitted

Table 1. Composition of Sample Solutions

Solution	Solute	Concentration / mol kg^{-1}	Solution	Solute	Concentration / mol dm^{-3}
CU-A	$Cu(CH_3COO)_2$	0.20	CO-A	$Co(CH_3COO)_2$	0.20
	CH_3COONa	1.58		CH_3COONa	1.58
	CH_3COOH	0.20		CH_3COOH	0.20
CU-B	$Cu(CH_3COO)_2$	0.10	CO-B	CH_3COONa	1.58
	H_6tpps	0.10		CH_3COOH	0.20
	CH_3COONa	0.50			
	CH_3COOH	0.20			
	NaOH	0.66			
CU-C	$Hg(CH_3COO)_2$	0.20	CO-C	$Hg(CH_3COO)_2$	0.20
	H_6tpps	0.20		H_6tpps	0.20
	CH_3COONa	1.61		CH_3COONa	1.61
	CH_3COOH	0.20		CH_3COOH	0.20
	NaOH	1.01		NaOH	1.01
			CO-D	$Hg(CH_3COO)_2$	0.0021
				H_6tpps	0.20
				CH_3COONa	1.61
				CH_3COOH	0.20
				NaOH	1.01

intensities as blank. The maximum gate time of the detection system of the present SF-EXAFS apparatus was 30 s, because accumulation of intensities of X-rays and dark currents on the position-sensitive photodiode array gave rise to saturation after 30 s. The apparent absorbance was obtained as $\ln(I_0/I)$.

First, aqueous solutions containing copper(II) sulfate, copper(II)-tpps, cobalt(II) perchlorate, hexaamminecobalt-(III) chloride, and cobalt(III)-tpps were each measured through the mixing chamber by the stopped-flow process in order to check the reproducibility of the measurements including the mixing process. The results obtained were compared with those obtained by the usual EXAFS and solution X-ray diffraction methods without the mixing process. Then, a cobalt(II) acetate solution (solution CO-A) and an acetate buffer (solution CO-B) were introduced to the stopped-flow cell through a mixing chamber. We found no disturbance caused by the mixing process.

The heterodinuclear intermediate, $[Hg(tpps)M^{II}]^{2-}$, was formed where solutions CU-C and CO-C were mixed with solutions CU-A and CO-A, respectively. We know from the kinetic data that after mixing the rate of formation of the reaction intermediate is fast enough that all the copper(II) or cobalt(II) ions form the intermediate 1 s after the mixing of the two solutions and that the intermediate exists for 10 s in the solution without significant decomposition. Thus, the 10 s measurement with a delay of 1 s after mixing was repeated several (> 100) times to accumulate the EXAFS data.

Formation of $[Co^{II}(tpps)]^{4-}$ was completed after 300 s of mixing. Therefore, the EXAFS data for the $[Co^{II}(tpps)]^{4-}$ complex were obtained by a 30 s measurement with a delay of 300 s after mixing an aqueous cobalt(II) acetate solution (solution CO-A) with an equivalent solution (solution CO-D) of porphyrin containing a small amount of mercury(II), and the 30 s measurement was repeatedly carried out 14 times during 1500 s after mixing of the solutions, because the $[Co^{II}(tpps)]^{4-}$ complex was present without significant oxidation in this period.

Background absorption other than that of K-shell absorption was estimated by the least-squares fitting Victoreen formula to the pre-edge data, and then subtracted from the total absorption in the post-edge region by extrapolation. The smooth K-shell absorption μ_0 was evaluated by fitting a smooth curve to the observed absorption spectrum using a sixth- or eighth-order polynomial function. The EXAFS pattern $\chi(k)$ was then extracted and normalized as

$$\chi(k) = \{\mu(k) - \mu_0(k)\}/\mu_0(k), \tag{10}$$

where k is the photoelectron wave vector and given as $2\pi\{2m(E-E_0)\}^{1/2}/h$. The parameter E represents the energy of the incident X-rays. The threshold energy of a K-shell electron, E_0, was selected as the position of the inflection point of the edge jump in each sample. Other notations have the usual meanings. The $\chi(k)$ values weighted by k^3 were converted to the radial structure function $F(r)$ as

$$F(r) = (1/2\pi)^{1/2} \int_{k_{min}}^{k_{max}} k^3\chi(k)W(k)\exp(-2ikr)\mathrm{d}k, \tag{11}$$

where $W(k)$ is the window function of the Hanning type.[27]

The model function $\chi(k)_{calcd}$ is given by the single-electron and single-scattering theory[28–31] as

$$\chi(k)_{calcd} = \sum \{n_j/(kr_j^2)\}\exp(-2\sigma_j^2k^2 - 2r_j/\lambda) \times Fj(\pi,k)\sin(2kr_j + \alpha_j(k)), \tag{12}$$

where $F_j(\pi,k)$ is the backscattering amplitude from each of n_j scatterers j at distance r_j from the X-ray absorbing atom. The parameter σ_j is the Debye–Waller factor, λ is the mean free path of the photoelectron and $\alpha_j(k)$ is the total scattering phase shift experienced by the photoelectron. The values of $F_j(\pi,k)$ and $\alpha_j(k)$ in Eq. 12 were quoted from the literature.[32,33] The structure parameters were determined in the k-space by comparing the Fourier filtered $k^3\chi(k)$ curve with the model function to minimize the error-square sum $\Sigma k^6(\chi(k)_{obsd} - \chi(k)_{calcd})^2$. The E_0 and λ values were evaluated from EXAFS spectra of standard samples. The parameters were then used as constants in the course of the subsequent structure analysis of unknown samples, while the r, σ, and n values were optimized as variables.

3. 4. Copper(II) Complexes. Figure 1a shows the extracted EXAFS oscillations $\chi(k)$ weighted by k^3 of the copper(II) complexes. The radial structure functions $F(r)$ uncorrected for the phase shift are depicted in Fig. 1b; these were obtained by the Fourier transformation of $k^3\chi(k)$ values in Fig. 1a. The first intense peaks around 150 pm in the $|F(r)|$ curves are due to the Cu–O and/or Cu–N bonds within the copper(II) complexes. The $[Hg(tpps)Cu]^{2-}$ intermediate and the $[Cu(H_2O)_6]^{2+}$ ion locate the position of the first peak at 154 pm and the $[Cu(tpps)]^{4-}$ complex at 143 pm, showing the different structure of the $[Cu(tpps)]^{4-}$ complex.

The structure parameters, r, σ, and n, of the copper(II) complexes in the first coordination sphere were finally determined by a least-squares calculation applied to the Fourier filtered $k^3\chi(k)$ values in the region $4.5\times10^{-2} < k/\mathrm{pm}^{-1} < 8.0\times10^{-2}$. The inverse Fourier transformation of the $F(r)$ values was carried out over the r range to include the main peak in the radial structure functions for each sample. To modify the values of the theoretical backscattering amplitude and phase shift, the E_0 and λ values were estimated in advance from EXAFS spectra of an aqueous copper(II) sulfate solution involving the $[Cu(H_2O)_6]^{2+}$ ion of known structure.[34] The Cu–O bond length within the $[Cu(H_2O)_6]^{2+}$ ion was also allowed to vary in order to check the reproducibility of the value; the Cu–O bond length obtained agrees well with the literature value.[34] Thus, the E_0 and λ values are well approximated in the present study. The r, σ, and n values for the acetato and porphyrinato complexes were then refined by adopting the E_0 and λ values thus determined. The best fit values are listed in Table 2. The solid lines calculated using the parameter values obtained reproduce well the experimental points, as depicted in Fig. 1c.

An EXAFS analysis by using SR of copper(II) acetate in an acetate buffer has evidenced an axially-elongated octahedral structure of the copper(II) ion.[35] Thus, in the course of the refinement of the structure parameters of the copper(II)

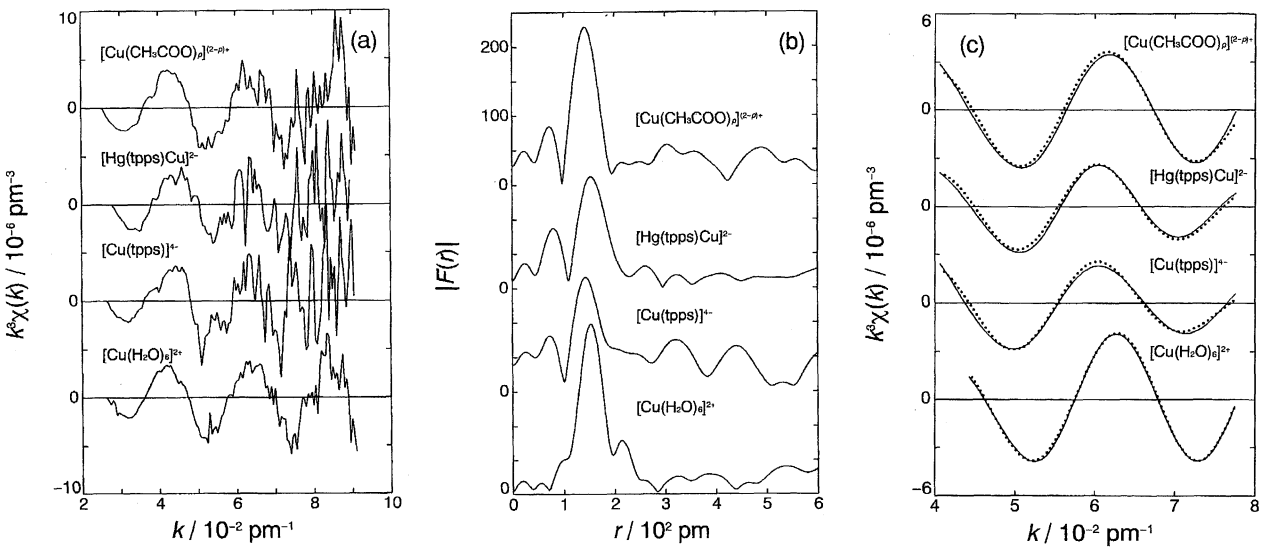

Fig. 1. (a) The EXAFS spectra in the form of $k^3\chi(k)$ for the copper(II) solutions. (b) The Fourier transforms $|F(r)|$ of the $k^3\chi(k)$ values shown in (a), uncorrected for the phase shift. (c) The Fourier filtered $k^3\chi(k)$ curves for the copper(II) solutions. The observed values are shown by dots and calculated ones using parameter values in Table 2 are shown by solid lines.

Table 2. Structure Parameters for the Copper(II) and Cobalt(II)/(III) Complexes in Water[a)]

Complex	Interaction	r/pm	σ/pm	n
Copper(II) complexes				
$[Cu(CH_3COO)_p]^{(2-p)+}$	$Cu–O_{eq}$	196 (1)	5.5 (0.3)	4[b)]
	$Cu–O_{ax}$	225 (3)	8.9 (0.7)	2[b)]
$[Hg(tpps)Cu]^{2-}$	$Cu–N_{eq}$	204 (1)	8.0[b)]	2[b)]
	$Cu–O_{eq}$	195 (1)	8.2[b)]	2[b)]
	$Cu–O_{ax}$	238 (2)	16.4 (0.7)	2[b)]
$[Cu(tpps)]^{4-}$	Cu–N	200 (1)	8.0 (0.6)	3.8 (0.2)
$[Cu(H_2O)_6]^{2+}$	$Cu–O_{eq}$	196 (1)	8.1 (0.2)	4[b)]
	$Cu–O_{ax}$	229 (3)	11.8 (0.4)	2[b)]
Cobalt(II)/(III) complexes				
$[Co^{II}(CH_3COO)_p]^{(2-p)+}$	$Co^{II}–O$	212 (1)	8.4 (0.1)	6.4 (0.1)
$[Hg(tpps)Co^{II}]^{2-}$	$Co^{II}–N$	212 (2)	1.3 (0.2)	2[b)]
	$Co^{II}–O$	221 (2)	1.3 (0.2)	3.6 (0.3)
$[Co^{II}(tpps)]^{4-}$	$Co^{II}–N$	203 (1)	2.7 (0.4)	4[b)]
	$Co^{II}–O$	215 (1)	2.7 (0.4)	2.3 (0.1)
$[Co^{II}(H_2O)_6]^{2+}$	$Co^{II}–O$	210 (1)	6.9 (0.3)	6[b)]
$[Co^{III}(tpps)]^{3-}$	$Co^{III}–N$	189 (1)	1.0 (5.7)	4[b)]
	$Co^{III}–O$	197 (2)	1.0 (5.7)	1.8 (0.1)
$[Co^{III}(NH_3)_6]^{3+}$	$Co^{III}–N$	194 (1)	5.6 (0.2)	6[b)]

a) Standard deviations of curve fits are given in parentheses. b) The values were kept constant during the calculations.

acetato complexes, the numbers of the $Cu–O_{eq}$ and $Cu–O_{ax}$ bonds were kept constant at 4 and 2, respectively. The determined $Cu–O_{eq}$ and $Cu–O_{ax}$ bond lengths are practically the same as those in $[Cu(H_2O)_6]^{2+}$ within experimental uncertainties. Under the present conditions, the copper(II) ions form the di-, tri-, and tetraacetato complexes on the basis of the stability constants of the copper(II) acetato complexes so far reported.[36] Four equatorial positions of the copper(II) ion seem to be occupied by acetate ions and/or water molecules, and two water molecules are interacting in the axial position.

The number of the Cu–N bonds in the $[Cu(tpps)]^{4-}$ complex converged to almost 4; thus, there should be no $Cu–OH_2$ interaction in the axial positions of the copper(II) ion. The Cu–N bond length is 200(1) pm and is in good agreement with the length determined by SR[35] and in the crystalline phase (5,10,15,20-tetraphenylporphyrinato and tetrapropylporphyrinato complexes).[37,38]

For the determination of the local structure around the copper(II) ion in the $[Hg(tpps)Cu]^{2-}$ intermediate, both a square-planar structure and an axially-elongated octahedral structure were examined. The error squares sum and R-factor were 0.76 pm^{-6} and 7.6% for the square-planar structure, and 0.28 pm^{-6} and 4.6% for the axially-elongated octahedral structure, respectively. Thus, the latter structure better reproduced the observed data than the former. The Cu–N bond length in the intermediate was determined to be 204(1)

pm. The Cu–O interactions were also observed in the intermediate, and acetate ions may bind to the copper(II) ion.

The reaction scheme and structure of the copper(II) complexes is shown in Fig. 2. The copper(II) ions in an acetate buffer are present as a mixture of acetato complexes, which have an axially-elongated octahedral structure. The mercury(II) ions also exist as a mixture of acetato complexes but the structure is four-coordinate tetrahedral.[35] The mercury(II) acetato complex reacts with H_2tpps^{4-} to form the heterodinuclear mercury(II) porphyrinato complex, in which each mercury(II) ion combines with two N atoms of $tpps^{6-}$ and an acetate ion.[35] Upon mixing copper(II) ion with an equivalent solution containing homodinuclear mercury(II)-porphyrinato complex, the heterodinuclear reaction intermediate $[Hg(tpps)Cu]^{2-}$ is formed. The coordination geometry around the copper(II) ion in the intermediate is axially-elongated octahedral. If we simply assume that the nonbonding N···N distance in the porphyrin ring does not change at the formation of the heterodinuclear intermediate and the N–Cu–N bond in the final $[Cu(tpps)]^{4-}$ product is linear, the copper(II) ion in the intermediate should be at least 40 pm off from the porphyrin plane. The reaction intermediate is decomposed to the square-planar $[Cu(tpps)]^{4-}$ complex and a four-coordinated mercury(II) acetato complex. The Cu–N bond length in the $[Cu(tpps)]^{4-}$ complex is 200 pm. The Cu-N bond length within the intermediate is longer than that in the product. The present EXAFS study directly shows elongation of the Cu–N bond in the short-lived unstable intermediate compared to that in the product. No significant change in the Cu–O bond was observed in the $[Hg(tpps)Cu]^{2-}$ complex compared with the reactant acetato complexes. This fact may be caused by the stability of the copper(II) ion owing to the Jahn–Teller effect in the distorted octahedral structure.

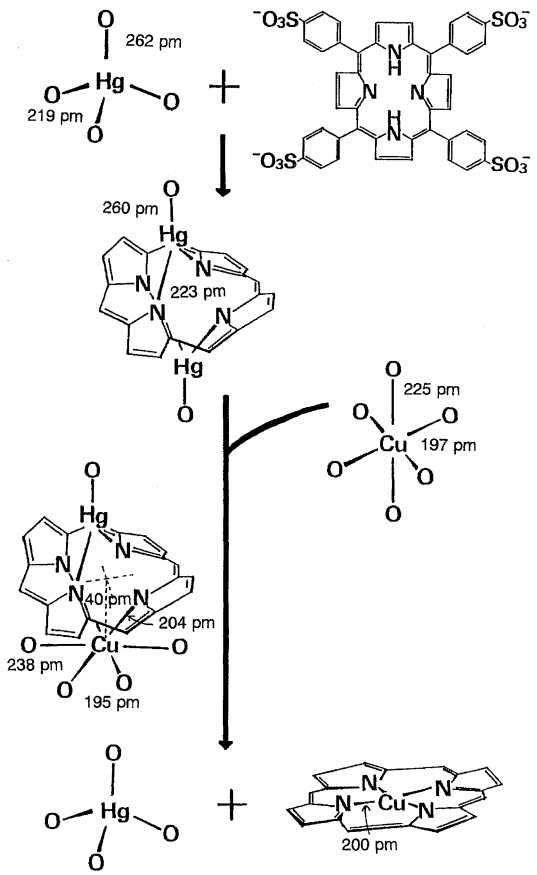

Fig. 2. Reaction scheme and bond length variation of complexes in the course of the metal substitution.

3. 5. Cobalt(II) and Cobalt(III) Complexes. Figures 3a and 3b depict the extracted Co *K*-edge EXAFS spectra in the form of $k^3\chi(k)$ and their Fourier transforms, respectively. The first peaks in the $|F(r)|$ curves in Fig. 3b are due to the Co–N and/or Co–O bonds in the first coordination sphere of the cobalt(II) and cobalt(III) ions. The intense peaks in the $|F(r)|$ curves of the cobalt(III) complexes appear around 145 pm, while those of the cobalt(II) complexes are located at an *r*-value larger than 150 pm. This is due to the smaller size of the cobalt(III) ion than that of the cobalt(II) ion. The peak position of $[Co^{II}(tpps)]^{4-}$ is 153 pm, which is significantly smaller than the 174 pm of $[Hg(tpps)Co^{II}]^{2-}$ and the 166 pm of $[Co^{II}(H_2O)_6]^{2+}$. This fact indicates that the structure of the $[Co^{II}(tpps)]^{4-}$ complex is significantly different from those of the other cobalt(II) complexes.

The r, σ, and n values of the metal complexes in the first coordination sphere were finally determined by a least-squares calculation applied to the Fourier filtered $k^3\chi(k)$ values in the k-space ($4.5\times10^{-2} < k/\mathrm{pm}^{-1} < 9.5\times10^{-2}$). The standard samples are aqueous solutions involving the $[Co^{II}(H_2O)_6]^{2+}$ and $[Co^{III}(NH_3)_6]^{3+}$ ions. The Co^{II}–O and Co^{III}–N bond lengths finally obtained were 210(1) and 194(1) pm, respectively. The Co^{II}–O bond length agrees well with that determined by the solution X-ray diffraction[34] and the Co^{III}–N distance with those found in crystalline $[Co^{III}(NH_3)_6]Cl_3$ and $[Co^{III}(NH_3)_6]I_3$.[39,40]

The structure parameters for the acetato and porphyrinato complexes were optimized as independent variables except for the number of the Co–N bonds. The cobalt(II) and cobalt(III) ions are expected to fully interact with the four nitrogen atoms of the porphyrin in $[Co^{II}(tpps)]^{4-}$ and $[Co^{III}(tpps)]^{3-}$. Thus, the number of Co^{II}–N and Co^{III}–N bonds was fixed to be 4. Also, the number of the Co^{II}–N bonds in the $[Hg(tpps)Co^{II}]^{2-}$ intermediate was kept constant at the value of 2, because in the homodinuclear $[Hg_2(tpps)]^{2-}$ complex each mercury(II) ion is coordinated to two nitrogen atoms.[34] The parameters finally obtained are given in Table 2. Figure 3c shows the agreement between the experimental and calculated $k^3\chi(k)$ curves.

An n value of practically six was obtained for the cobalt(II) ion in an acetate buffer. Similar to the copper(II) ions in an acetate buffer, the cobalt(II) ions are expected to be present as a mixture of $[Co(H_2O)_6]^{2+}$ and cobalt(II) acetato complexes. Thus, the structure of $[Co(CH_3COO)_p]^{(2-p)+}$ ($p = 1,2\cdots$) is octahedral.

The cobalt(II) ion in the $[Hg(tpps)Co^{II}]^{2-}$ intermediate exhibits coordination number 6, i.e., there exist two Co^{II}–N and four Co^{II}–O (water and/or acetate) bonds with bond lengths of 212 and 221 pm, respectively. The cobalt(II) ion in the intermediate is situated in an octahedral environment.

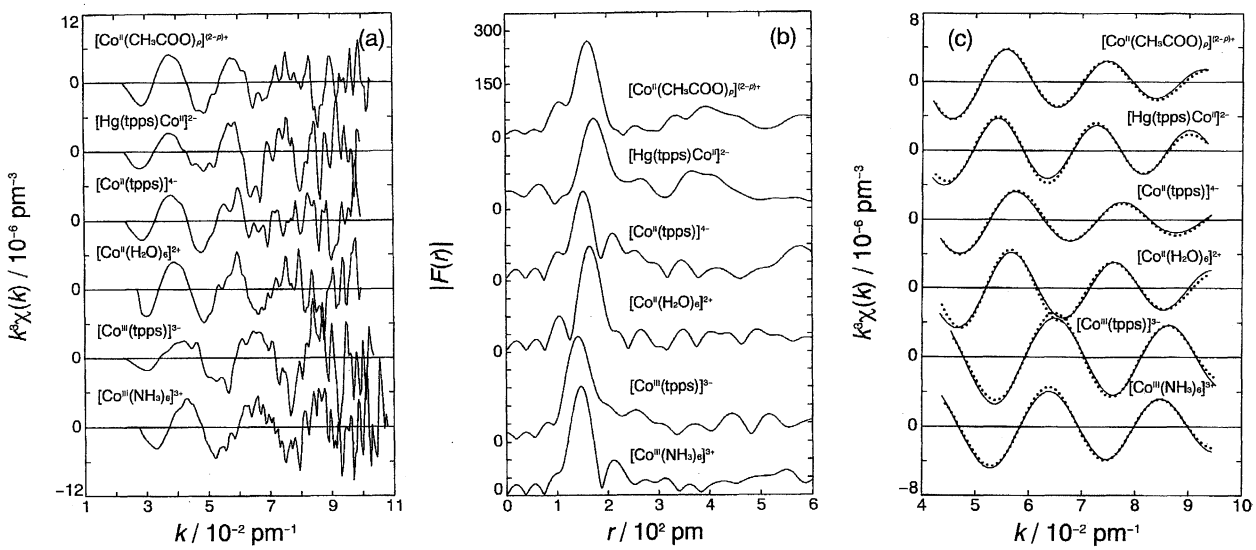

Fig. 3. (a) The EXAFS spectra in the form of $k^3\chi(k)$ for the cobalt(II) and cobalt(III) solutions. (b) The Fourier transforms $|F(r)|$ of the $k^3\chi(k)$ values shown in (a), uncorrected for the phase shift. (c) The Fourier filtered $k^3\chi(k)$ curves for the cobalt(II) and cobalt(III) solutions. The observed values are shown by dots and calculated ones using parameter values in Table 2 are shown by solid lines.

The number of the Co^{II}–O (water and/or acetate) bonds in the [Co^{II}(tpps)]$^{4-}$ complex was found to be practically 4. The complex has an octahedral structure with two Co^{II}–N bonds.

The n value was nearly two for the Co^{III}–O bonds within [Co^{III}(tpps)]$^{3-}$, and the cobalt(III) ion is coordinated with four nitrogen atoms of porphyrin and two additional oxygen atoms. Thus, the structure of the complex is six-coordinate octahedral.

Figure 4 summarizes the structure of the cobalt complexes. The cobalt(II) acetato complex reacts with the homodinuclear mercury(II) porphyrinato complex in an acetate buffer and the heterodinuclear reaction intermediate [Hg(tpps)Co^{II}]$^{2-}$ is formed. The coordination geometry around the cobalt(II) ion in the intermediate and in the reactant is six-coordinate octahedral. The Co^{II}–N and Co^{II}–O bond lengths in the intermediate are 212 and 221 pm, respectively. The Co^{II}–N bond length is slightly shorter than that within the octahedrally solvated cobalt(II) ion in nitrogen-donor solvents, e.g., 214 pm in 3-methylpyridine, 216 pm in 4-methylpyridine[41] and 217 pm in 1,3-propanediamine and in n-propylamine.[42] By the decomposition of the reaction intermediate, the six-coordinate octahedral [Co^{II}(tpps)]$^{4-}$ complex is formed, the Co^{II}–N and Co^{II}–O bond lengths in the complex being 203 and 215 pm, respectively. The Co^{II}–N bond length within the [Hg(tpps)Co^{II}]$^{2-}$ intermediate is 9 pm longer than that within the [Co^{II}(tpps)]$^{4-}$ product. The electronic configuration of the cobalt(II) ion in the [Hg(tpps)Co^{II}]$^{2-}$ intermediate is expected to be high-spin, while the cobalt(II) ion in the [Co^{II}(tpps)]$^{4-}$ complex is in a low-spin state. The different Co^{II}–N bond length mainly results from the different spin states of the cobalt(II) ions in the two complexes, because a low-spin cobalt(II) ion generally has a smaller ionic radius than a high-spin one.[43] The Co^{II}–O (water and/or acetate) bond length of 221 pm in the intermediate is 9 pm longer than that in the reactant and 6 pm longer than that in

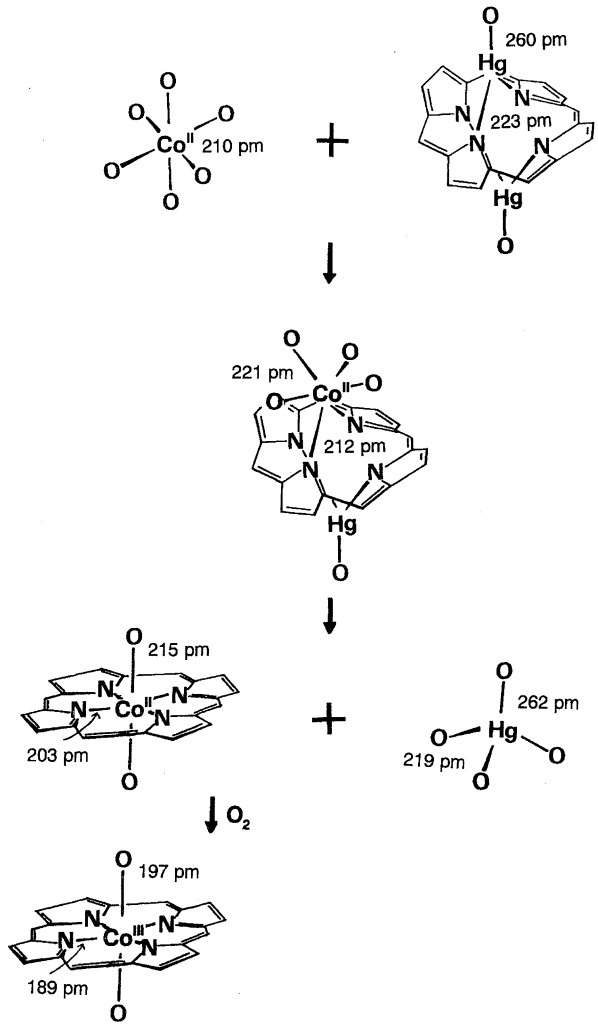

Fig. 4. Scheme of the metal substitution and oxidation reactions and bond length variation of species.

the product. The longer Co^{II}–O bond in the intermediate as compared to that in the reactant and in the product should be responsible for the instability of the intermediate. Finally, the $[Co^{II}(tpps)]^{4-}$ complex is oxidized by dissolved oxygen to give $[Co^{III}(tpps)]^{3-}$, which has an octahedral structure with the Co^{III}–N and Co^{III}–O bond lengths of 189 and 197 pm, respectively.

4. Concluding Remarks

The success for the determination of the structure of the heterodinuclear reaction intermediate $[Hg(tpps)M^{II}]^{2-}$ is certainly owing to the suitable systems selected. The good selection means not only finding out a reaction intermediate having a lifetime suitable for a method of structure determination but also building up a suitable experimental condition to obtain the maximum concentration of the reaction intermediate on the basis of the kinetic data.

The local structure around the mercury(II) ion in the $[Hg(tpps)M^{II}]^{2-}$ intermediate is not open at present because our SF-EXAFS apparatus does not have enough energy resolution in the X-ray energy range larger than 10 keV. The reactivity of the heterodinuclear reaction intermediate should be discussed on the basis of local structures around two metal centers in the intermediate. We are now planning to determine the structure of a heterodinuclear reaction intermediate appearing during a ligand-transfer reaction between two complexes of different metal ions, both of which are suitable for our SF-EXAFS method. The direct structural analysis of a heterodinuclear reaction intermediate is important in another aspect, i.e., the formation of a heterodinuclear reaction intermediate should occur through an inner-sphere electron transfer process.

The sampling time of X-ray intensities of our SF-EXAFS technique is on the order of 1 s. Application of SR will come to expand this method to a shorter time range and also to a wider X-ray energy range and a better accuracy of the measurements.

Chemical reactions are initiated by mixing of two reactant solutions in a stopped-flow cell in SF-EXAFS measurements. The mixing process has a deadtime of a few ms; thus, faster reactions should be initiated by other methods.

Finally, we like to emphasize that the structure analysis of reaction intermediates in the time domain requires sufficient knowledge from both instrumental and reaction kinetic points of view.

The authors thank Mr. Shintaro Ohnishi of Ritsumeikan University, Prof. Masaaki Tabata of Saga University, Dr. Yasuhiro Inada and Prof. Shigenobu Funahashi of Nagoya University for their collaboration in the present work. We also acknowledge the financial support of Institute for Molecular Science in Okazaki and the Ministry of Education of Japan.

References

1 "Time-Resolved Diffraction," ed by J. R. Hellwell and P. M. Rentzepis, Oxford Univ. Press, New York (1997).

2 P. Coppens, D. V. Fomitchev, M. D. Carducci, and K. Culp, *J. Chem. Soc., Dalton Trans.*, **1998**, 865.

3 H. Ohtaki, *Pure Appl. Chem.*, **65**, 2589 (1993).

4 Y. Inada, S. Funahashi, and H. Ohtaki, *Rev. Sci. Instrum.*, **65**, 18 (1994).

5 H. Ohtaki, Y. Inada, S. Funahashi, M. Tabata, K. Ozutsumi, and K. Nakajima, *J. Chem. Soc., Chem. Commun.*, **1994**, 1023.

6 K. Ozutsumi, S. Ohnishi, H. Ohtaki, and M. Tabata, *Z. Naturforsch., B*, **53b**, 469 (1998).

7 T. Matsushita and R. P. Phizackerley, *Jpn. J. Appl. Phys.*, **20**, 2223 (1981).

8 R. P. Phizackerley, Z. U. Rek, G. B. Stephenson, S. D. Conradson, K. O. Hodgson, T. Matsushita, and H. Oyanagi, *J. Appl. Crystallogr.*, **16**, 220 (1983).

9 A. M. Flank, A. Fontaine, A. Jucha, M. Lemonnier, and C. Williams, *J. Phys. (Paris)*, **43**, L315 (1982).

10 A. M. Flank, A. Fontaine, A. Jucha, M. Lemonnier, D. Raout, and C. Williams, *Nucl. Instrum. Methods*, **208**, 651 (1983).

11 T. Matsushita, H. Oyanagi, S. Saigo, U. Kaminaga, H. Hashimoto, H. Kihara, N. Yoshida, and M. Fujimoto, *Jpn. J. Appl. Phys.*, **25**, L523 (1986).

12 S. Saigo, H. Oyanagi, T. Matsushita, H. Hashimoto, Y. Yoshida, M. Fujimoto, and T. Nagamura, *J. Phys. (Paris), Colloq.*, **47**, C8-555 (1986).

13 Y. Yoshida, T. Matsushita, S. Saigo, H. Oyanagi, H. Hashimoto, and M. Fujimoto, *J. Chem. Soc., Chem. Commun.*, **1990**, 354.

14 H. W. Huang, W. H. Liu, and J. A. Buchanan, *Nucl. Instrum. Methods*, **205**, 375 (1983).

15 H. W. Huang, W. H. Liu, T. Y. Teng, and X. F. Wang, *Rev. Sci. Instrum.*, **54**, 1488 (1983).

16 D. M. Mills, A. Lewis, A. Harootunian, J. Huang, and B. Smith, *Science*, **223**, 811 (1984).

17 Y. Inada and S. Funahashi, *Z. Naturforsch., B*, **52b**, 711 (1997).

18 Y. Inada, H. Hayashi, S. Funahashi, and M. Nonura, *Rev. Sci. Instrum.*, **68**, 2973 (1997).

19 N. Kagayama, M. Sekiguchi, Y. Inada, H. D. Takagi, and S. Funahashi, *Inorg. Chem.*, **33**, 1881 (1994).

20 B. Chance, R. Fischetti, and L. Powers, *Biochemistry*, **22**, 3820 (1983).

21 L. Powers, J. L. Sessler, G. L. Woolery, and B. Chance, *Biochemistry*, **23**, 5519 (1984).

22 L. X. Chen, M. K. Bowman, P. A. Montano, and J. R. Norris, *J. Am. Chem. Soc.*, **115**, 4373 (1983).

23 D. J. Thiel, P. Līvinš, E. A. Stern, and A. Lewis, *Nature*, **362**, 40 (1993).

24 M. Tabata and M. Tanaka, *Trends Anal. Chem.*, **10**, 126 (1991).

25 M. Tabata and W. Miyata, *Chem. Lett.*, **1991**, 785.

26 M. Tabata, W. Miyata, and N. Nahar, *Inorg. Chem.*, **34**, 6492 (1995).

27 F. J. Harris, *Proc. IEEE*, **66**, 51 (1978).

28 D. E. Sayers, E. A. Stern, and F. W. Lytle, *Phys. Rev. Lett.*, **27**, 1204 (1971).

29 E. A. Stern, *Phys. Rev. B*, **10**, 3027 (1974).

30 E. A. Stern, D. E. Sayers, and F. W. Lytle, *Phys. Rev. B*, **11**, 4836 (1975).

31 B. Lengeler and P. Eisenberger, *Phys. Rev. B*, **21**, 4507 (1989).

32 B.-K. Teo and P. A. Lee, *J. Am. Chem. Soc.*, **101**, 2815

(1979).
33 A. D. McKale, B. W. Veal, A. P. Pailinkas, C. K. Chan, and G. S. Knapp, *J. Am. Chem. Soc.*, **110**, 3767 (1988).
34 H. Ohtaki, T. Yamaguchi, and M. Maeda, *Bull. Chem. Soc. Jpn.*, **49**, 701 (1976).
35 M. Tabata and K. Ozutsumi, *Bull. Chem. Soc. Jpn.*, **67**, 1608 (1994).
36 A. E. Martell and R. M. Smith, "Critical Stability Constants," Plenum, New York (1977).
37 I. Moustakali and A. Tulinsly, *J. Am. Chem. Soc.*, **95**, 6811 (1964).
38 E. B. Fleischer, C. K. Miller, and L. E. Webb, *J. Am. Chem. Soc.*, **86**, 2342 (1964).
39 G. J. Kruger and E. C. Reynhardt, *Acta Crystallogr., Sect. B*, **B34**, 915 (1978).
40 N. E. Kime and J. A. Ibers, *Acta Crystallogr., Sect. B*, **B25**, 168 (1969).
41 M. Kurihara, K. Ozutsumi, and T. Kawashima, *J. Solution Chem.*, **24**, 719 (1995).
42 S. Aizawa, S. Iida, K. Matsuda, and S. Funahashi, *Inorg. Chem.*, **35**, 1338 (1996).
43 R. D. Shannon, *Acta Crystallogr., Sect. A*, **A32**, 751 (1976).

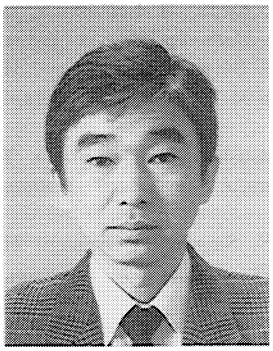

Kazuhiko Ozutsumi was born in 1957 in Ibaraki prefecture, Japan. He graduated from Kanazawa University in 1979. He obtained M. Sc. degree from Kanazawa University in 1981 and Dr. Sc. degree in 1984 from Tokyo Institute of Technology. He became a Research Associate of the Tokyo Institute of Technology in 1985 and he was a Research Associate at the Institute of Molecular Science of the Okazaki National Research Institutes from 1986 to 1987. He was appointed as an Assistant Professor of University of Tsukuba in 1988 and as an Associate Professor of Ritsumeikan University in 1995. His research interests include structural studies of metal complexes by using X-ray diffraction and EXAFS methods as well as thermodynamic studies of complexation in various solvents.

Hitoshi Ohtaki was born in 1932 in Tokyo, Japan. He graduated from Nagoya University in 1955 and obtained M. Sc. and Dr. Sc. degrees in 1957 and 1961, respectively, from Nagoya University. He became a Research Associate of the Tokyo Institute of Technology in 1959. He studied complex equilibria in solution under the supervision of Prof. L. G. Sillén, Stockholm, Sweden, as a postdoctoral research fellow from 1961 to 1964. He was appointed Lecturer of Nagoya University in 1965 and promoted to Associate Professor in 1967. In 1970 he moved back to Tokyo Institute of Technology as an Associate Professor, and then became a Full Professor in 1973. As Professor of the Institute of Molecular Science of the Okazaki National Research Institutes from 1988, he was the Director of the Coordination Chemistry Laboratories. On his retirement in 1993 he became Professor Emeritus of the Tokyo Institute of Technology and the Graduate University for Advanced Studies. He was appointed as Professor of Ritsumeikan University and the Director of the Institute of Science and Engineering of Ritsumeikan University in 1994. His research interests cover various areas of solution chemistry, especially structural chemistry in solution, including studies on solvent, solvated ions and complexes existing in solution by means of X-ray diffraction; EXAFS and neutron diffraction methods have been occasionally employed as well. Thermodynamic studies on solution equilibria have long been another major area of his study. Molecular dynamics simulation studies on dissolution and nucleation process of crystals have improved the knowledge of chemistry of ionic solvation and crystal growth from the dynamic viewpoint. He received Matsunaga Prize in 1976, Tejima Memorial Award in 1989, Takei Prize in 1990, National Medal of Purple Ribbon in 1995 and the Kato Memorial Lectureship of Electrochemical Society of Japan in 1999.